US Army Corps of Engineers

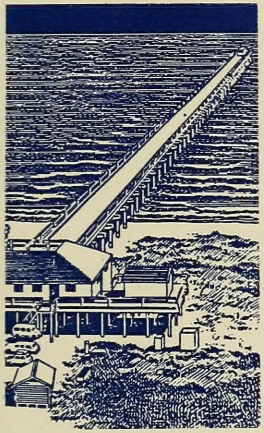

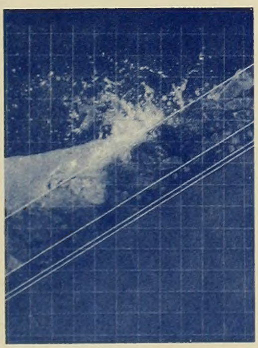

TECHNICAL REPORT CERC-88-5

APPROXIMATE UPPER LIMIT OF IRREGULAR WAVE RUNUP ON RIPRAP

by

John P. Ahrens, Martha S. Heimbaugh

Coastal Engineering Research Center

DEPARTMENT OF THE ARMY
Waterways Experiment Station, Corps of Engineers
PO Box 631, Vicksburg, Mississippi 39180-0631

May 1988

Final Report

Approved For Public Release; Distribution Unlimited

Prepared for US Army Engineer District, Detroit
PO Box 1027, Detroit, Michigan 48231-1027

and

US Army Engineer District, Jacksonville
PO Box 4970, Jacksonville, Florida 32232-0019

Unclassified

SECURITY CLASSIFICATION OF THIS PAGE

REPORT DOCUMENTATION PAGE		Form Approved OMB No 0704-0188 Exp. Date: Jun 30, 1986
1a. REPORT SECURITY CLASSIFICATION Unclassified	1b. RESTRICTIVE MARKINGS	
2a. SECURITY CLASSIFICATION AUTHORITY	3. DISTRIBUTION/AVAILABILITY OF REPORT Approved for public release; distribution unlimited.	
2b. DECLASSIFICATION/DOWNGRADING SCHEDULE		
4. PERFORMING ORGANIZATION REPORT NUMBER(S) Technical Report CERC-88-5	5. MONITORING ORGANIZATION REPORT NUMBER(S)	
6a. NAME OF PERFORMING ORGANIZATION USAEWES Coastal Engineering Research Center	6b. OFFICE SYMBOL (If applicable) WESCW	7a. NAME OF MONITORING ORGANIZATION
6c. ADDRESS (City, State, and ZIP Code) PO Box 631 Vicksburg, MS 39180-0631	7b. ADDRESS (City, State, and ZIP Code)	
8a. NAME OF FUNDING/SPONSORING ORGANIZATION See reverse.	8b. OFFICE SYMBOL (If applicable)	9. PROCUREMENT INSTRUMENT IDENTIFICATION NUMBER
8c. ADDRESS (City, State, and ZIP Code) See reverse.	10. SOURCE OF FUNDING NUMBERS PROGRAM ELEMENT NO. / PROJECT NO. / TASK NO. / WORK UNIT ACCESSION NO	

11. TITLE (Include Security Classification)

Approximate Upper Limit of Irregular Wave Runup on Riprap

12. PERSONAL AUTHOR(S)

Ahrens, John P.; Heimbaugh, Martha S.

13a. TYPE OF REPORT	13b. TIME COVERED	14. DATE OF REPORT (Year, Month, Day)	15. PAGE COUNT
Final report	FROM ____ TO ____	May 1988	33

16. SUPPLEMENTARY NOTATION

Available from National Technical Information Service, 5285 Port Royal Road, Springfield, VA 22161.

17. COSATI CODES			18. SUBJECT TERMS (Continue on reverse if necessary and identify by block number)
FIELD	GROUP	SUB-GROUP	Irregular waves; Prediction method; Revetments; Riprap; Runup

19. ABSTRACT (Continue on reverse if necessary and identify by block number)

This report describes methods to calculate the approximate upper limit of runup on riprap revetments caused by irregular wave action. A formula to predict the maximum runup is developed from one laboratory study and compared to data from a second study. The formula is found to fit the data of both studies quite well. A slightly improved version of the formula is then developed by combining the data from both studies. The improved formula has little or no systematic error associated with structure slope, water depth, or wave conditions and is easy to use. Errors between predicted and observed elevations of the maximum runup had a root mean square value of approximately 12 percent.

20. DISTRIBUTION/AVAILABILITY OF ABSTRACT	21. ABSTRACT SECURITY CLASSIFICATION	
☒ UNCLASSIFIED/UNLIMITED ☐ SAME AS RPT. ☐ DTIC USERS	Unclassified	
22a. NAME OF RESPONSIBLE INDIVIDUAL	22b. TELEPHONE (Include Area Code)	22c. OFFICE SYMBOL

DD FORM 1473, 84 MAR — 83 APR edition may be used until exhausted. All other editions are obsolete.

SECURITY CLASSIFICATION OF THIS PAGE

Unclassified

8a. NAME OF FUNDING/SPONSORING ORGANIZATION (Continued).

US Army Engineer District, Detroit; and
US Army Engineer District, Jacksonville

8c. ADDRESS (CITY, STATE, AND ZIP CODE) (Continued).

PO Box 1027
Detroit, MI 48231-1027 and

PO Box 4970
Jacksonville, FL 32232-0019

PREFACE

Summarized herein are important findings obtained from unpublished model studies conducted by the Coastal Engineering Research Center (CERC) for the US Army Engineer District, Detroit (NCE), and the US Army Engineer District, Jacksonville (SAJ).

This report was prepared at the US Army Engineer Waterways Experiment Station (WES). The data were compiled and analyzed by Mr. John P. Ahrens, Oceanographer, and Ms. Martha S. Heimbaugh, Civil Engineer, both of CERC. The data were collected by Messrs. Martin Titus and Louis Meyerly and Ms. Karen Zirkel, Civil Engineering Technicians, CERC.

General supervision was provided by Dr. James R. Houston, Chief, CERC, Mr. Charles C. Calhoun, Jr., Assistant Chief, CERC, Dr. Charles L. Vincent, Program Manager, CERC, and Mr. C. E. Chatham, Jr., Chief, Wave Dynamics Division, CERC.

COL Dwayne G. Lee, CE, was Commander and Director of WES during the preparation and publication of this report. Dr. Robert W. Whalin was Technical Director.

CONTENTS

APPROXIMATE UPPER LIMIT OF IRREGULAR WAVE RUNUP ON RIPRAP

PART I: INTRODUCTION

1. In many locations riprap is the preferred type of shore protection against wave attack. The two reasons for this are the low cost and high durability of stone, and the effectiveness of randomly placed stone, because of its roughness and porosity, in dissipating wave energy and attenuating runup. Because of these reasons, riprap has been the most studied type of revetment, and its performance is well documented.

2. Runup is one of the most important factors affecting the design of revetments exposed to wave action. Generally, riprap revetments are designed so that little or no runup exceeds the top of the protection. Because of the inherent complexity of natural wave trains and the interaction of incident waves and the return flow of previous runup on a rough, porous slope, it is difficult to predict the upper limit of wave uprush on riprap. This report summarizes the most important results from two unpublished studies, and presents formulas to calculate the approximate limit of wave runup. Both studies included laboratory tests of riprap exposed to irregular wave action. The formulas can be used to compute the elevation to which protection needs to be extended to prevent exceedance by runup or to estimate the potential severity of wave overtopping.

PART II: SOURCES OF DATA, TEST SETUPS, AND TEST CONDITIONS

3. The sources of data for this report came from model studies conducted primarily for two US Army Corps of Engineer Districts, Detroit (NCE) and Jacksonville (SAJ).

4. Model studies conducted for NCE were to investigate wave runup on riprap-protected dredge disposal dikes in the Great Lakes. The scope of this study was expanded to include an unusually wide range of water depths at the toe of the structure d_s , zero-moment wave heights H_{mo} , and period of peak energy density of the incident wave spectrum T_p . By expanding the scope of this study beyond the immediate problems occurring on the Great Lakes, the opportunity to develop a general wave-runup prediction method was provided. A summary of test conditions for both the NCE and SAJ studies is given in Table 1, and data collected on both studies are tabulated in Appendix A.

Table 1

Summary of Test Conditions

Study	Embankment Slope	d_s cm	H_{mo} cm	T_p cm	W_{50} g	Armor Unit Weight g/cm^3	Number of Tests
NCE	1 on 2	11.9-38.5	4.9-17.5	1.02-4.74	189	2.65	40
SAJ	1 on 3	19.0-23.8	3.0-10.5	1.39-1.46	63.3-67.0	2.55	21
SAJ	1 on 4	19.0-23.8	3.2-10.3	1.39-1.49	56.9	2.55	8

5. A 1- on 2- (1 vertical:2 horizontal) structural slope was used in the NCE study. Plywood roughened with glued on pea gravel was used as the supporting slope and simulated the impermeable core of the dike. This slope was covered with a filter layer of Sioux Quartzite 5.5 cm thick. The range of weight for this stone was from 6 to 41 g with a median weight of 18 g. Riprap armor stone was placed by hand on top of the filter layer. Armor stones were composed of Kimmswick Limestone with a range of weight from 144 to 233 g with a median weight of 189 g. The armor layer was 10 cm thick. Figure 1 shows a profile view of the model structure, and Figure 2 shows a plan view of the test setup.

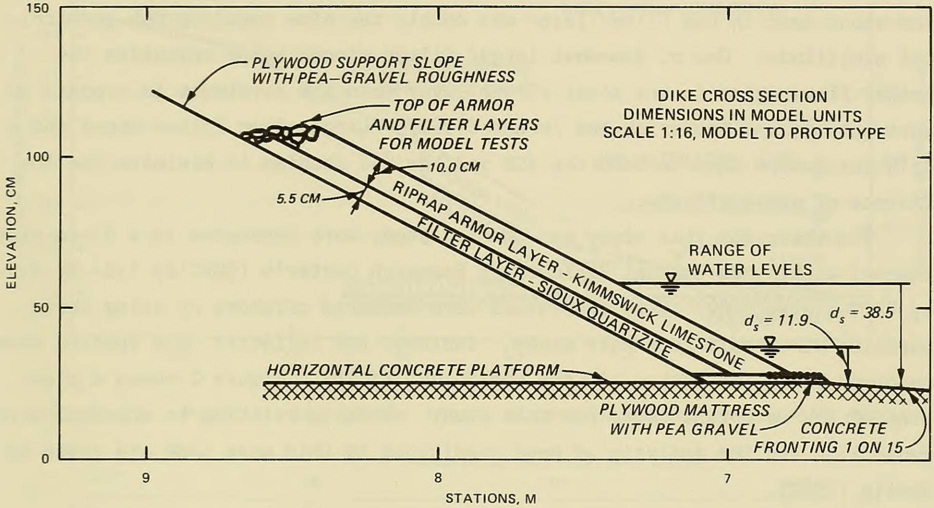

Figure 1. Profile view of structure tested during NCE study

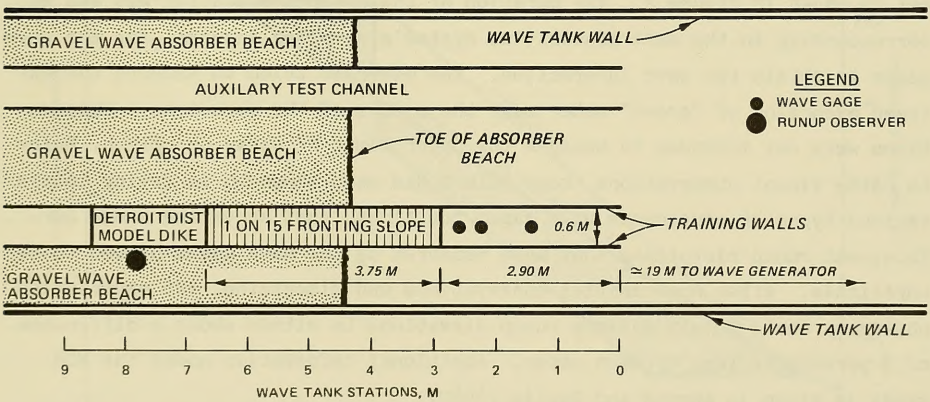

Figure 2. Plan view of test setup for NCE study

6. The model was constructed at a nominal 1:16 (model:prototype) undistorted Froude scale. The influence of scale effects at this large a scale was considered to be small. To further reduce the possibility of scale effects, the stone used in the filter layer was double the size required for geometrical similitude. Use of somewhat larger filter stones helps establish the proper flow-regime in the model filter layer when the revetment is exposed to wave action; see Broderick and Ahrens (1982). Large-sized filter stone and a 1:16 scale were used in both the NCE and the SAJ studies to minimize the influence of scale effects.

7. Tests for this study and the SAJ study were conducted in a 61-cm-wide channel within the Coastal Engineering Research Center's (CERC's) 1.2- by 4.6- by 42.7-m wave tank. Wave conditions were measured offshore by using three parallel wire-resistance wave gages. Incident and reflected wave spectra were resolved using the method of Goda and Suzuki (1976). Figure 2 shows a plan view of the wave tank setup for this study. Details relating to spectral wave generation and the analysis of wave conditions in this wave tank are given by Seelig (1980).

8. Maximum wave runup elevations were obtained by visual observations made by an experienced observer, and quantified by using a point gage. The observer stood immediately adjacent to the structure in a wave absorber channel as shown in Figure 2. The duration of the runup observation was 256 sec, corresponding to the data acquisition system's sampling interval for the wave gages to obtain the wave information. The observer tried to measure the extreme excursion of "green" water near the middle of the structure. Observations were not intended to measure the upper limit of spray or splash. Prior to using visual observations, some effort had been expended in trying to use various types of continuous wave gages positioned just above the armor surface, but runup elevations that were measured by the wave gages proved to be unreliable. After some initial observations and discussion, two experienced observers could obtain maximum runup elevations to within about a difference of 3 percent or less of each other. Additional information about the NCE study is given in Ahrens and Seelig (1980).

9. The SAJ study was conducted to investigate the stability of and wave runup on riprap to be used to protect Herbert Hoover Dike on Lake Okeechobee, Florida. Two structural slopes were tested during this study, 1 on 4 and 1 on 3. Figure 3 shows a profile view of the 1-on-4 slope tested. Figure 4 shows

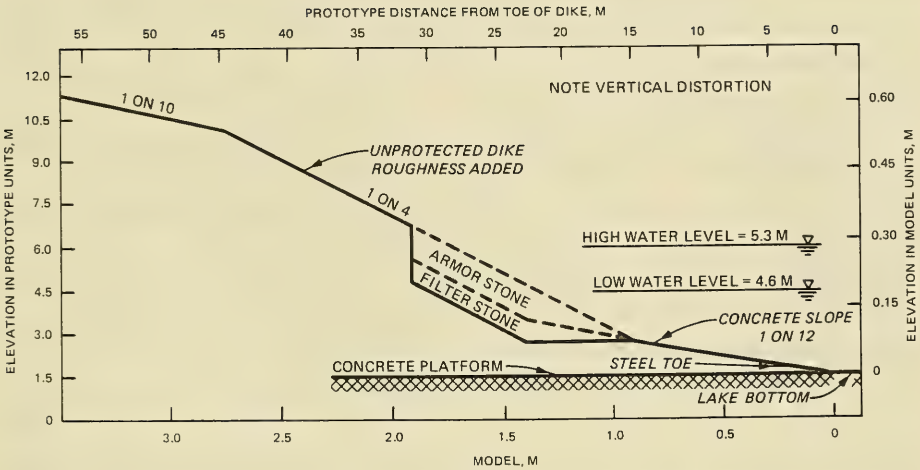

Figure 3. Profile view of the 1 on 4 structure tested during SAJ study

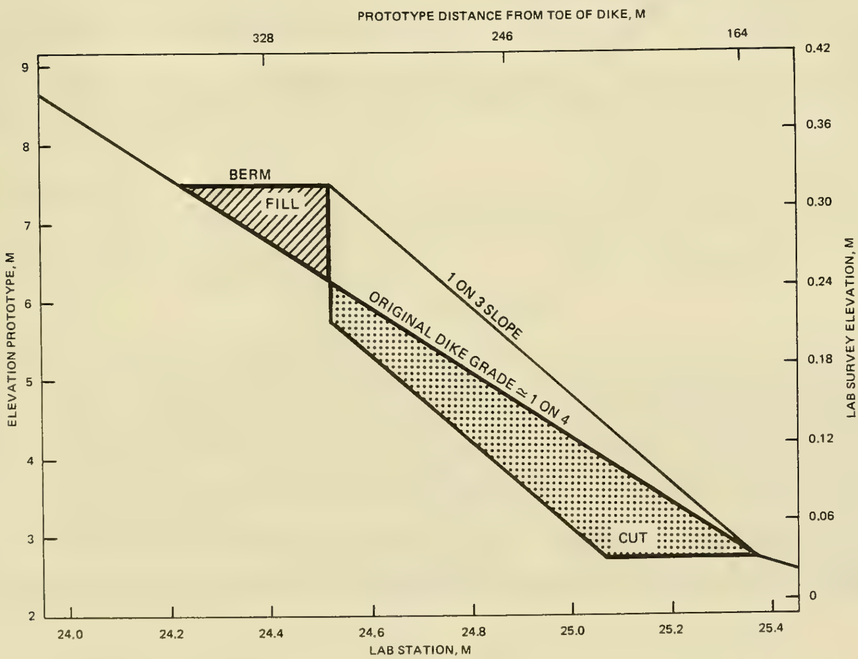

Figure 4. Profile view of cut and fill used to construct a 1 on 3 dike embankment slope for SAJ study

the cut and fill strategy used to construct a 1-on-3, riprap-protected slope on the embankment. Figure 5 shows a profile view of the 1-on-3 slope tested and the location of the wave gages. Figure 6 shows a plan view of the test setup.

10. Since the armor stone planned to protect the dike was marine limestone to be quarried in Florida, this type of stone was used in the model tests. This stone has a density of 2.55 g/cm^3. The armor stone had a median weight which ranged from about 57 to 67 g during the course of the study (see Table 1). Filter stone had a median weight of about 12 g and a layer thickness of 2.5 cm. Additional details relating to test procedures and setup are given in Ahrens and Zirkle (1982).

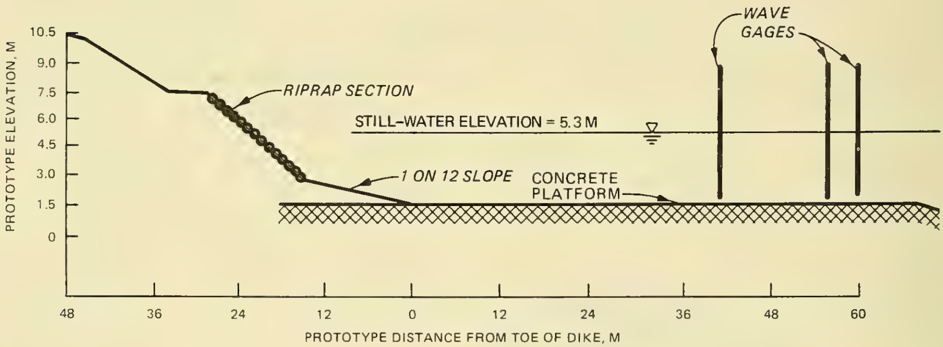

Figure 5. Profile view of 1-on-3, riprap-protected slope and offshore wave gages

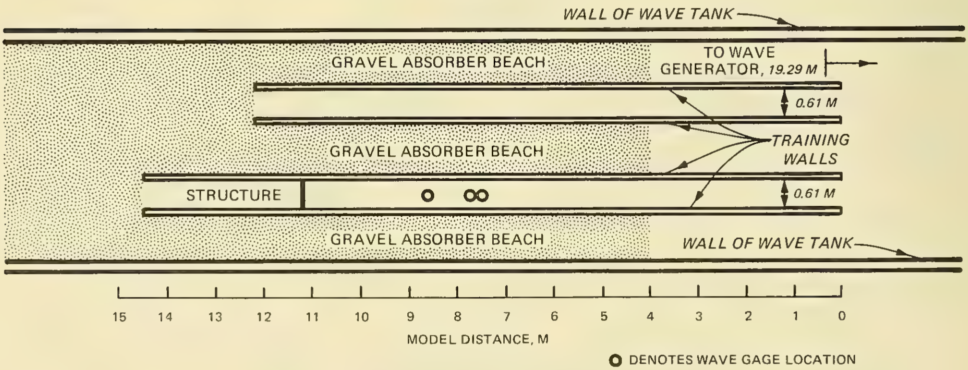

Figure 6. Plan view of SAJ test setup

PART III: ANALYSIS OF DATA AND DEVELOPMENT OF RUNUP FORMULAS

11. The biggest difficulty with analyzing the data from the NCE study was making accurate estimates of the zero-moment wave height H_{mo} at the toe of the structure. In the NCE study the wave heights were measured offshore in a water depth 25 cm greater than at the toe of the structure. Due to shoaling and breaking, a wide range of offshore wave conditions can yield the same zero-moment wave height in shallow water. Therefore, the offshore wave height is not as useful as the wave height at the toe of the riprap structure. The wave conditions near the structure correlate well with the runup and often can be estimated accurately by depth-limited considerations. Originally in the NCE study the wave heights at the toe were estimated by using the method of Goda (1975) which accounts for shoaling and breaking of irregular waves. However, after scrutinizing the information generated by Goda's model, it was observed that for some situations the method yielded values of H_{mo}/d_s greater than 0.8 which is higher than has been observed in any of CERC's wave tank calibration tests. Because of this limitation, it was decided to try and develop another method to estimate H_{mo} at the toe of the structure.

12. Several methods were tested to account for the wave shoaling and breaking between the offshore gages and the toe of the structure. The method that worked best was a hybrid method which combined linear-wave shoaling with the relation given by Hughes (1984) as

$$\left[\frac{H_{mo}}{\left(L_p\right)^{3/4}}\right]_I = \left[\frac{H_{mo}}{\left(L_p\right)^{3/4}}\right]_O \qquad (1)$$

where

L_p = Airy wave length calculated at those depths for the period of peak energy density T_p

I and O = inshore and offshore water depths, respectively

From wave-tank calibration tests it has been found that the approximate limiting value for the zero-moment wave height is given by

$$\left(\frac{H_{mo}}{L_p}\right)_{max} = 0.10 \tanh\left(\frac{2\pi d_s}{L_p}\right) \qquad (2)$$

where d_s is the water depth at or near the structure toe. The procedure used to calculate the zero-moment wave height at the toe of the structure was to calculate the value by using both linear shoaling and Equation 1 and then taking the average of the two estimates. If the average exceeded the maximum value suggested by Equation 2, then that limiting value was used.

13. The ability of the above procedure to estimate H_{mo} in shallow water is demonstrated in Figure 7 using wave-tank calibration data collected

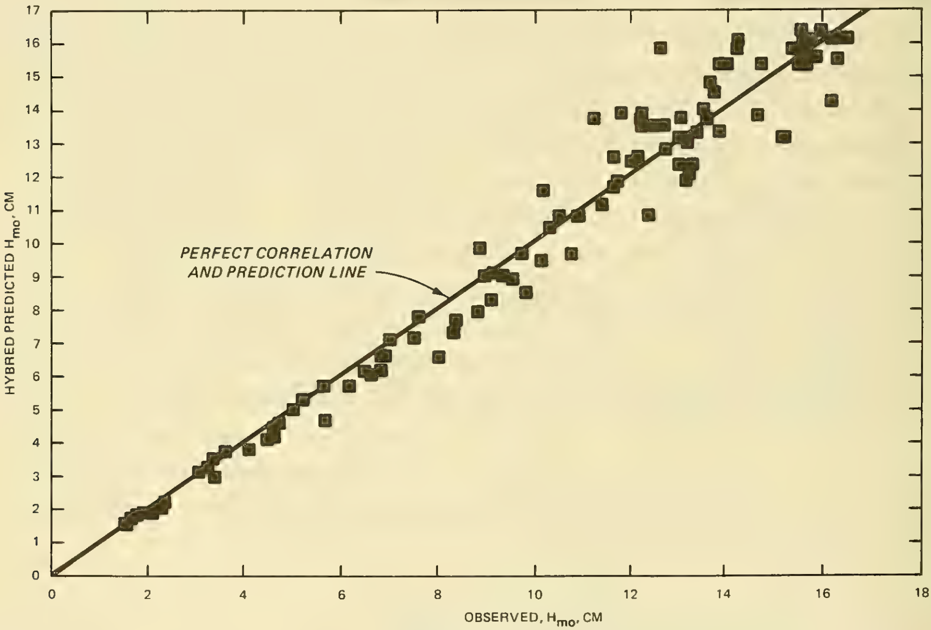

Figure 7. Predicted versus observed H_{mo} for tank calibration data

prior to a study of wave overtopping of a seawall (Ahrens, Heimbaugh, and Davidson 1986). This calibration data included a wide range of wave periods and an extensive amount of wave shoaling and breaking for many conditions between the offshore wave gages and an inshore gage located in front of a wave absorber beach. For the calibration data shown in Figure 7, the offshore water depth ranged from 61.9 to 66.2 cm; the inshore water depth ranged from 22.9 to 27.2 cm; the offshore H_{mo} ranged from 1.6 to 21.5 cm; the inshore H_{mo} ranged from 1.5 to 16.4 cm; and the period of peak energy density ranged from 1.75 to 3.00 sec. The hybrid method given above appears to work well for CERC calibration data because linear shoaling tends to overestimate inshore

H_{mo} while Equation 1 tends to underestimate inshore H_{mo} , and Equation 2 provides a logical limiting value on H_{mo} . Based on the success of the hybrid model in predicting known data, the model was applied to the NCE study to estimate H_{mo} at the toe of the structure. Subsequent analysis of predicted and observed maximum runup elevations suggests that the hybrid method makes good estimates of H_{mo} in shallow water.

14. The wide range of water depths tested in the NCE study had been included partly to investigate the influence of water depth on wave runup. This concern is strongly reflected in the discussion of wave runup in the Shore Protection Manual (1984). From previous studies it was known that runup would be strongly influenced by the surf condition on the structures (Ahrens and McCartney 1975), but it also seemed logical that the maximum runup would be dependent on the shape of the wave-height distribution and nonlinear effects. The last two influences would be very dependent on the water depth at the toe of the structure and the wave periods. To investigate the influence of surf characteristics on runup, the surf parameter for irregular waves ξ is defined as

$$\xi = \frac{\tan \theta}{\left(\frac{H_{mo}}{L_o}\right)^{1/2}} \tag{3}$$

where

$\tan \theta$ = tangent of the angle θ between the structure slope and the horizontal

$L_o = gT_p^2/2\pi$ = the deep-water wave length

g = the acceleration of gravity

When a runup model was formulated using the surf parameter, it was found to contain some systematic errors which could be related to the relative wave height H_{mo}/d_s . However, when a surf parameter was defined by using the local wave length, a model could be formulated which did not include systematic errors related to the relative wave height. The modified surf parameter ξ_L is defined

$$\xi_L = \frac{\tan \theta}{\left(\frac{H_{mo}}{L_p}\right)^{1/2}} \tag{4}$$

where

L_p = the Airy wave length calculated by using the water depth at the toe of the structure

d_s = the period of peak energy density, T_p

Runup is computed using the formula

$$\frac{R_{max}}{H_{mo}} = \frac{aS}{1.0 + bS} \tag{5}$$

where

R_{max} = elevation of maximum wave runup

S = surf parameter defined by either Equation 3 or 4 depending on the prediction method selected

a and b = dimensionless runup coefficients determined by regression analysis

Equation 5 has a form which is especially convenient and logical for predicting wave runup on rough porous slopes as shown by Ahrens and McCartney (1975), and, subsequently, by Seelig (1980) and US Army Corps of Engineers (1985). For the NCE data, using the modified surf parameter defined by Equation 4, the coefficients in Equation 5 were found to be $a = 1.062$ and $b = 0.153$.

15. By using the coefficients given above, Equation 5 does a good job of predicting R_{max} for both the NCE and SAJ studies. Figure 8 shows the predicted values of R_{max} versus the observed values of R_{max} by using different symbols to identify the two studies. The good fit to the NCE data is gratifying considering the problem related to estimating the H_{mo} at the toe of the structure. The good fit to the SAJ data is somewhat surprising considering that the thickness of the armor layer for the SAJ test was considerably thinner than the armor layer used in the NCE tests. In addition, the structural slopes tested for SAJ were 1 on 3 and 1 on 4 compared with a slope of 1 on 2 for the NCE tests. These findings indicate that the maximum runup may not be too sensitive to the armor-layer thickness, and that the surf parameter properly accounts for differences in the structural slopes. It should also be recalled that the runup coefficients were obtained from the NCE study so that the SAJ data provide a rather severe test for the runup model's predictive ability.

16. By lumping the data from the two studies together, somewhat better

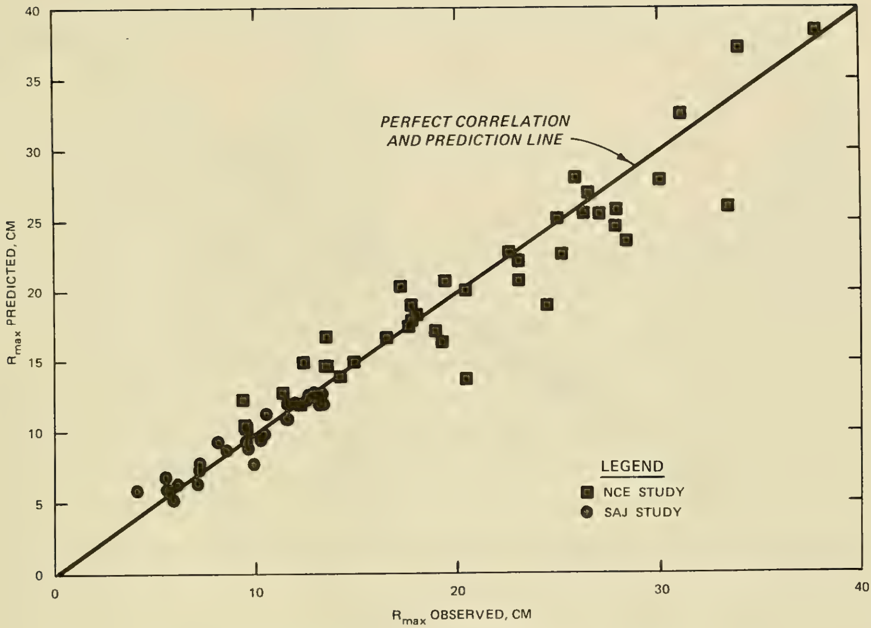

Figure 8. R_{max} predicted, using coefficients from NCE data, versus R_{max} observed, both NCE and SAJ studies

a and b runup coefficients can be determined. By using regression analysis on the combined data set, the improved coefficients are $a = 1.154$ and $b = 0.202$. A new scatter plot comparing predicted and observed values was prepared with the above coefficients, and Equation 5 was used to calculate the predicted values of maximum runup. The new scatter plot (see Figure 9) shows that the change in the runup coefficients caused very little change over the scatter plot shown in Figure 8. Even though there was little change in the scatter plot, the limiting value for R/H_{mo} dropped from 6.9 to 5.7; the limiting value for Equation 5 is given by the ratio of a to b .

17. To investigate systematic error in predicting the maximum runup and to identify possible ways to improve the prediction method based on the modified surf parameter ξ_L , a series of error plots was made. In these plots, the percent error %E in predicting the maximum runup is defined as

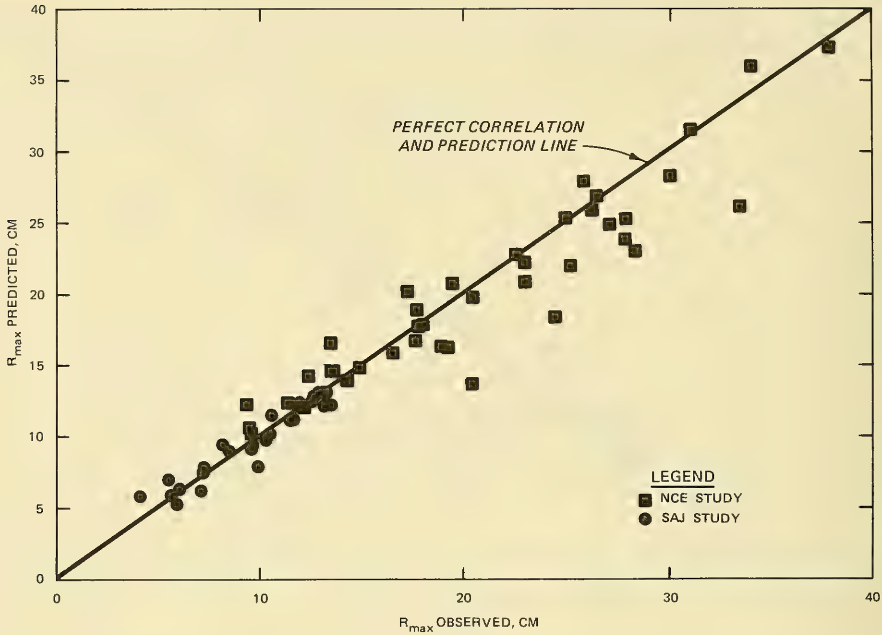

Figure 9. R_{max} predicted, using coefficients from both NCE and SAJ data, versus R_{max} observed for NCE and SAJ data

$$\%E = \frac{\left(R_{max}\right)_p - \left(R_{max}\right)_o}{R_{max_o}} \times 100 \qquad (6)$$

where the subscripts p and o indicate predicted and observed, respectively. The percent error is plotted versus ξ_L , ξ , d_s/L_p , H_{mo}/L_p , H_{mo}/d_s , $r(bar)/d_{50}$, and II, and cot θ in Figure 10a, b, c, d, e, f, g, and h, respectively, where r is the average armor-layer thickness and II is Goda's (1983) nonlinear parameter defined for irregular waves

$$II = \frac{\dfrac{H_{mo}}{L_p}}{\tan h^3\left(\dfrac{2\pi d_s}{L_p}\right)} \qquad (7)$$

The larger the value of II , the more nonlinear the waves with

$$\Pi \longrightarrow \frac{H_{mo}}{L_p} \text{ , for deep-water conditions}$$

and

$$\Pi \longrightarrow \frac{H_{mo} L_p^2}{\left(2\pi d_s\right)^3} \text{ , Ursell's parameter for shallow-water wave conditions}$$

Figure 10 shows little or no systematic error for the prediction method based on L_p . Figure 10 also shows that the percent error ranges from -33 to +44 percent, but that for most tests the error is within about ±10 percent.

18. Approximately 25 percent of the tests had a percent error greater than ±10 percent. Because of this, it may be useful in some critical or life-threatening situations to use a value of R_{max} greater than the expected value produced by Equation 5 when using the recommended coefficients. Figure 11 shows how the percent error which has been normalized by the standard deviation of the data set σ seems to have the shape of a normal distribution. To test this hypothesis, namely, that the percent error has a normal distribution, a Kolmogorov-Smirnov (K&S) test was performed. This test is used to determine whether or not the data deviate a statistically significant amount from the assumed normal distribution model (Cornell and Benjamin 1970).

19. The K&S test indicates that the normal distribution for error should be accepted at the 20-percent significance level. A 20-percent level is a more severe criterion than a 10-percent level as it indicates there is a 20-percent chance of rejecting a model which is in fact true, a Type I error. The 20-percent significance level is the most severe criterion commonly tabulated for the K&S tests. Recognizing that errors have a normal distribution provides an easy way to give more conservative estimates of R_{max} than is provided by a regression equation. Generally, about half the errors are above the regression curve and about half are below, so the curve represents a 50_ percent exceedance level. In Figure 12 a more conservative trend is shown above the regression curve. The conservative curve was generated by increasing the runup regression coefficient a by two standard deviations of the percent error, i.e.,

$$a_c \text{ (conservative a)} = a\,(1 + 2\sigma) = 1.143\,(1.0 + 2 \times 0.1286) = 1.437$$

The value of the runup coefficient b remains the same, i.e., $b = 0.202$.

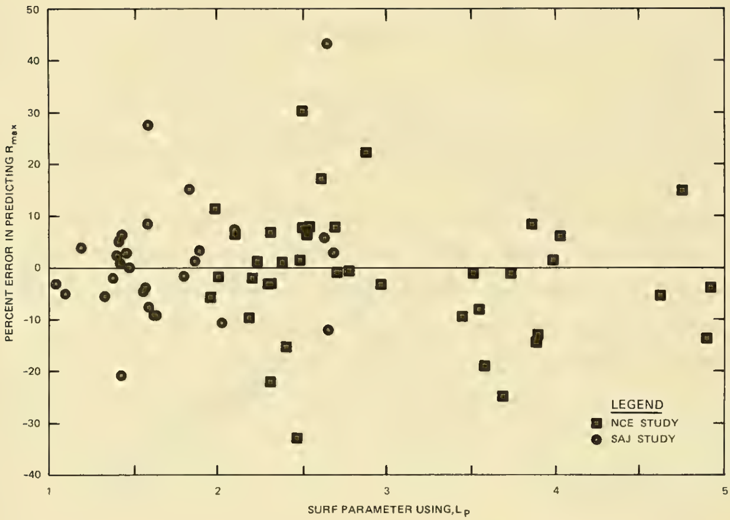

a. Percent error R_{max} versus surf parameter using L_p

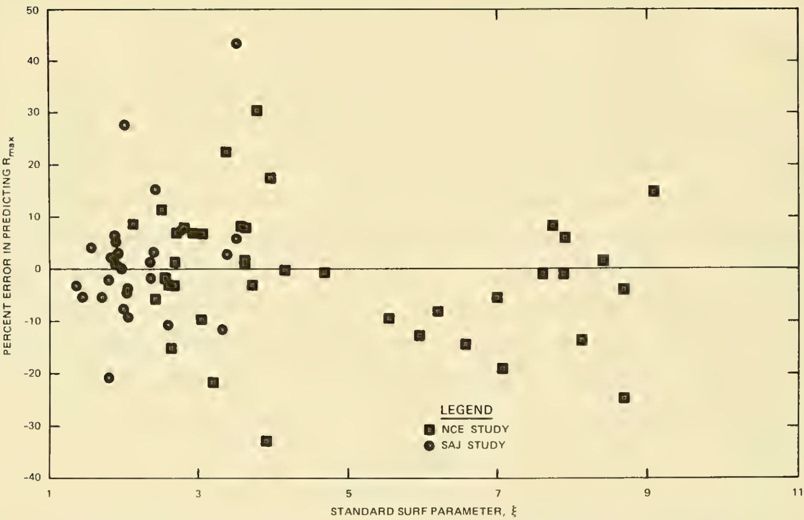

b. Percent error R_{max} versus standard surf parameter, ξ

Figure 10. Percent error in predicting R_{max} (Sheet 1 of 4)

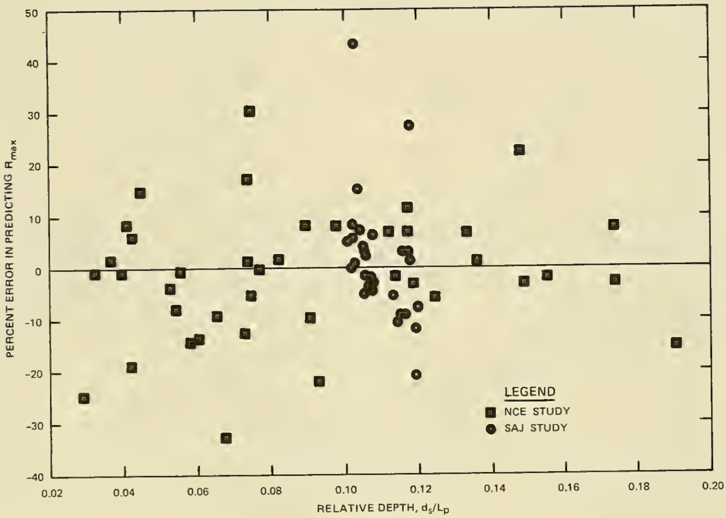

c. Percent error R_{max} versus relative depth, d_s/L_p

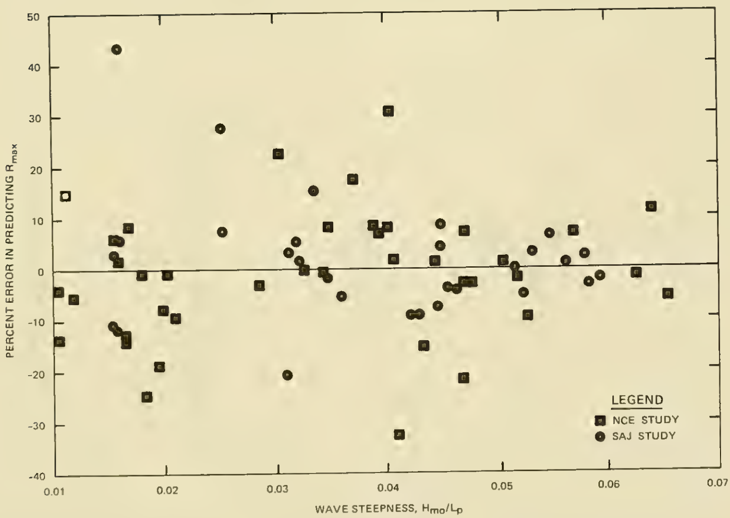

d. Percent error R_{max} versus steepness, H_{mo}/L_p

Figure 10. (Sheet 2 of 4)

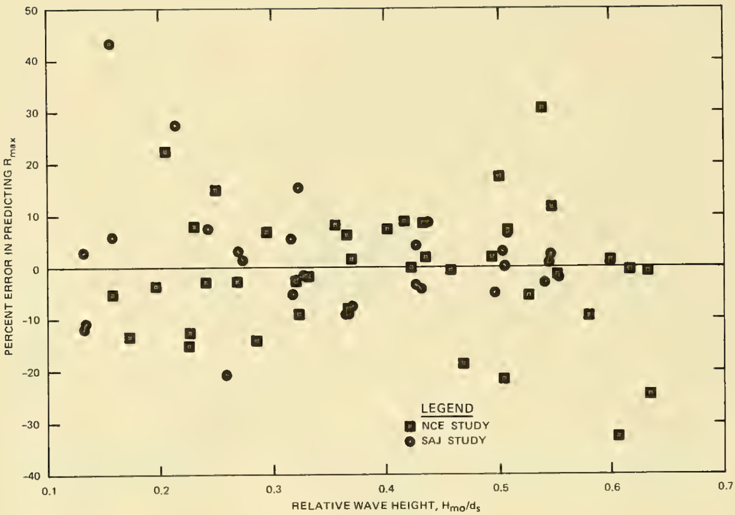

e. Percent error R_{max} versus wave height, H_{mo}/d_s

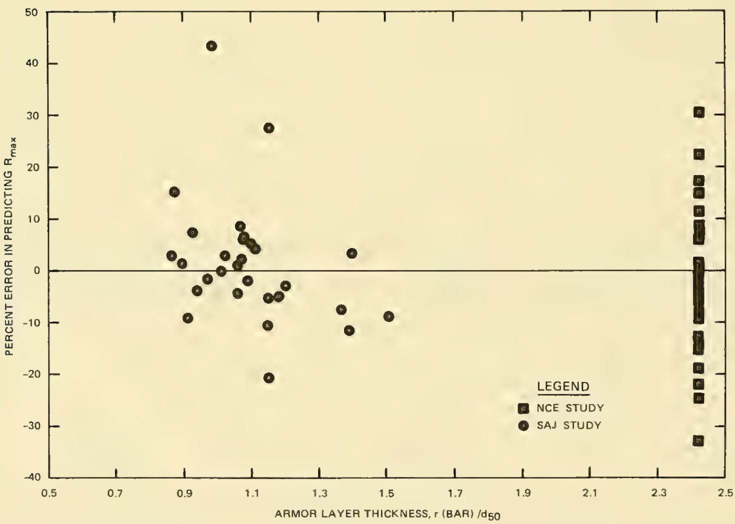

f. Percent error R_{max} versus armor-layer thickness, r(bar)/d_{50}

Figure 10. (Sheet 3 of 4)

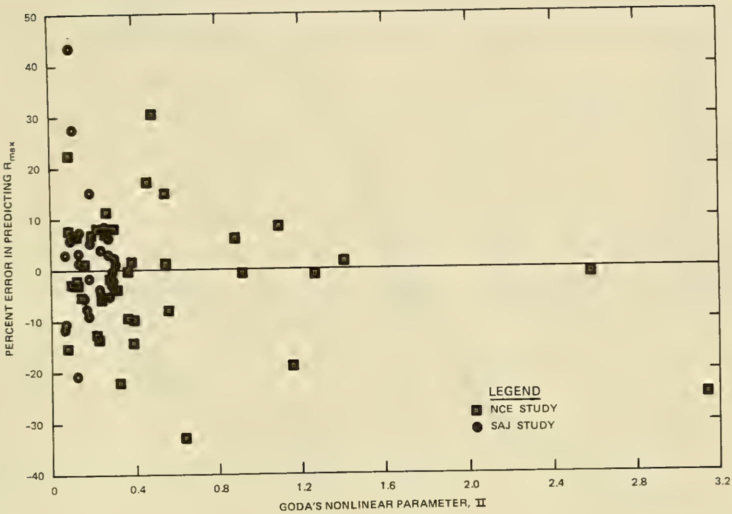

g. Percent error R_{max} versus Goda's nonlinear parameter, II

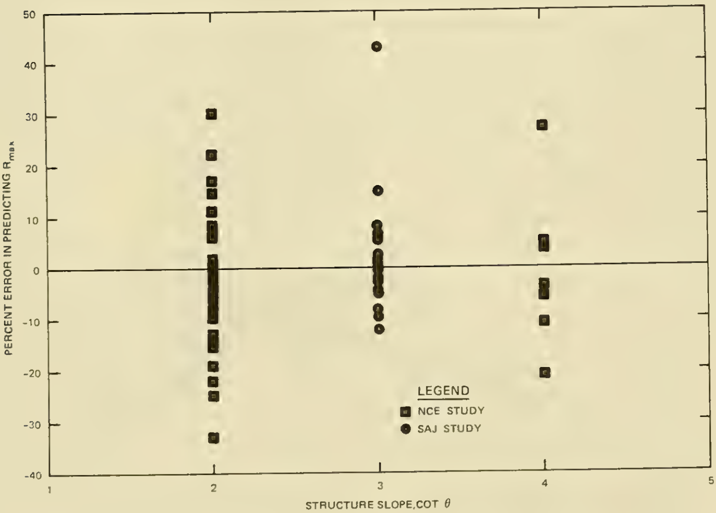

h. Percent error R_{max} versus structure slope, cot θ

Figure 10. (Sheet 4 of 4)

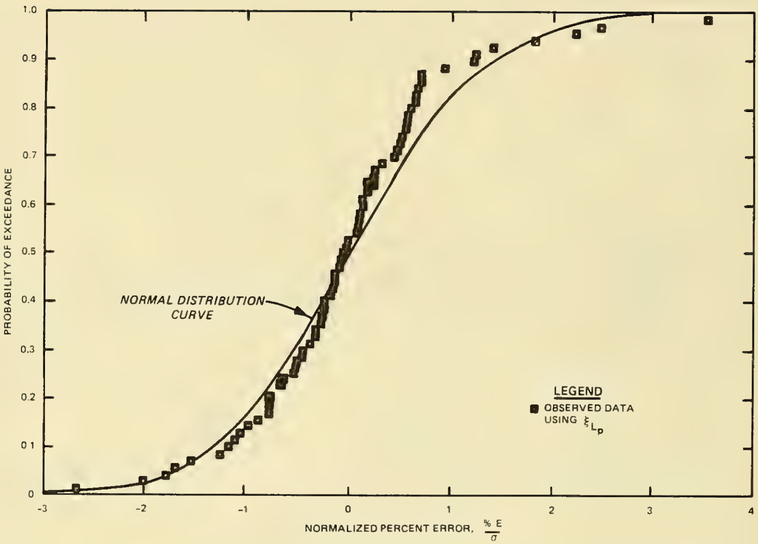

Figure 11. Normal distribution curve for ξ_{L_p} model data

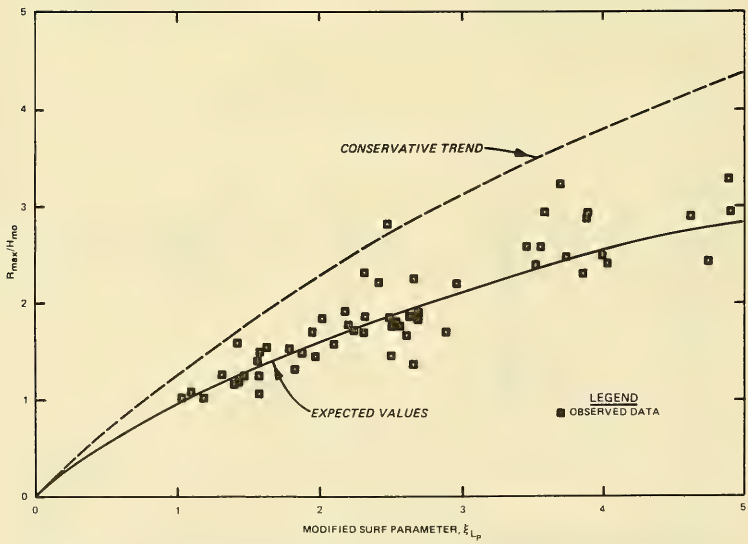

Figure 12. Expected value and more conservative trend curves for ξ_{L_p} model

It can be seen in Figure 12 that the new conservative runup curve provides a envelope for the observed data. The conservative curve would be expected to exceed about 97.7 percent of the data. An exceedance level of 97.7 percent is obtained from a standard normal distribution table for a value two standard deviations greater than the mean. Figure 12 helps confirm the method of choosing an envelope curve by showing only one observed value above the conservative curve. This is approximately what would be expected for a normal distribution with a sample size of 69. Other curves used to predict maximum runup could be constructed which would be more or less conservative than the example just provided. The degree of conservatism would be evaluated on the basis of the risk posed by waves overtopping the revetment.

20. Since the standard surf parameter has been frequently used to predict wave runup, it is useful to provide a prediction formula based on that method to allow comparison to earlier studies. Using Equation 3 to define the surf parameter in Equation 5, the runup coefficients were determined for the combined NCE and SAJ data sets as $a = 1.022$ and $b = 0.247$. Figure 13 shows the predicted and observed values of R_{max}/H_{mo} versus the standard surf parameter. It can be seen that the predicted values follow the trend of the observed data very well. Using the same method to evaluate errors as was used

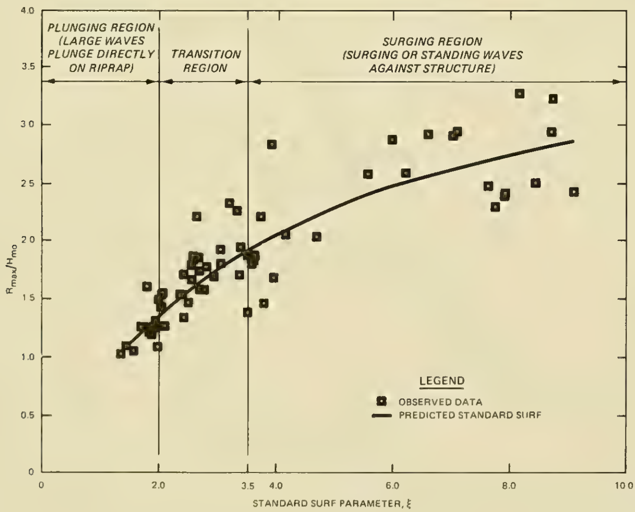

Figure 13. Comparison of the prediction of R_{max} using ξ

for the Equation 4 model, it was found that there were no systematic errors associated with the model which used the standard surf parameter. Figure 14 shows that the standarized percent errors for this model also seem to have a normal distribution. Performing the K&S test once again showed that these data were also normal at the 20-percent significance level and thus, could be assumed to have a normal distribution. Figure 15 shows the more conservative curve which could be expected to envelop 97.7 percent of the data and represents an increase of two standard deviations over the expected mean curve. The coefficients for this conservative curve are $a = 1.285$ and $b = 0.247$. Once again, this curve is only one of many more conservative curves that could be constructed depending upon the design situation. Using the runup coefficients with the standard surf parameter would be an easy way to estimate R_{max} using a small calculator. The more accurate model would require the calculation of L_p for use in the modified surf parameter which would be more difficult than calculating the deep-water wave length for the standard surf parameter.

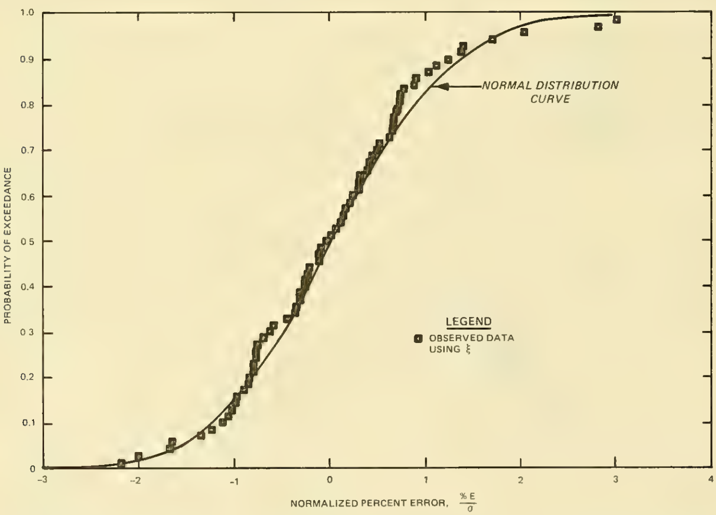

Figure 14. Normal distribution curve for ξ model data

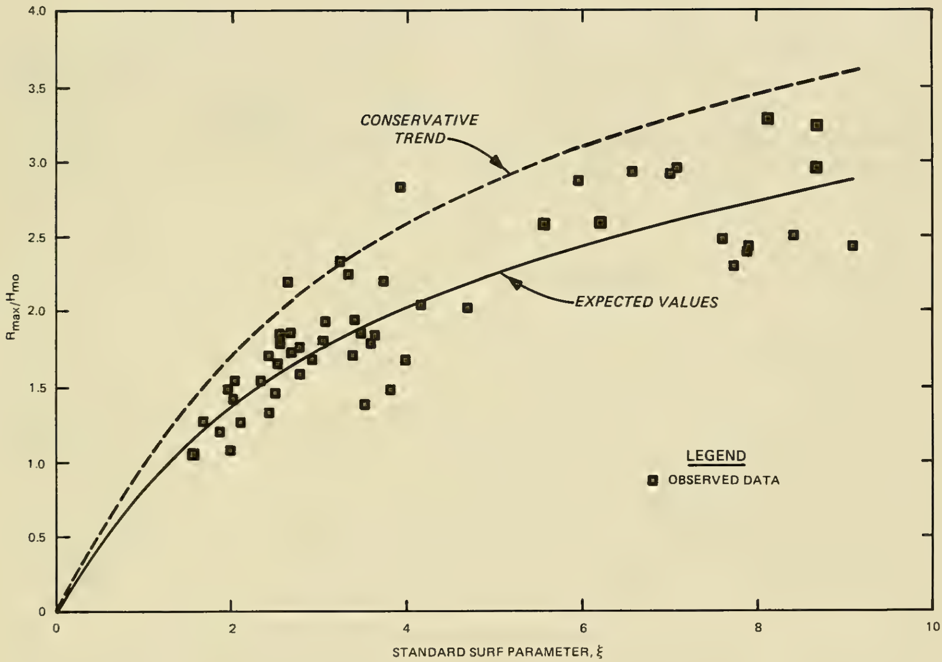

Figure 15. Expected value and more conservative trend curves for ξ model

PART IV: SUMMARY

21. All the equations presented within this report were developed from two unpublished laboratory studies. These equations provide an easy way to calculate the R_{max} of irregular waves on riprap-protected embankments. Table 2 summarizes the important information about two runup equations which

Table 2

Summarized Information for Maximum Runup Formula, Equation 5

Formula Category	Wave Length Used	Surf Parameter Used in Equation 5	Runup Coefficients	Variance Explained	σ , Standard Deviation of Percent Error
Recommended	L_p	ξ_L (Equation 4)	a = 1.154 b = 0.202	$R^2 = 0.843$	12.3
Alternative	L_o	ξ(Equation 3)	a = 1.022 b = 0.247	$R^2 = 0.817$	12.9

represent the most accurate existing method to determine the approximate upper limit of wave uprush on a riprap revetment. The two equations are presented as a recommended method and an alternate method to compute R_{max} . The recommended method has little or no systematic error such as might be associated with the influence of water depth or nonlinear effects and is slightly more accurate than the alternate method. The alternative method is easier to calculate and can serve as a "rule of thumb" estimate. In Table 2 the runup coefficients are to be used in the general runup equation (Equation 5) by using either the standard or modified surf parameter as noted. A method was developed which provides a reasonable way to make the predicted values of R_{max} more conservative. It was found that the errors in predicting R_{max} have a normal distribution, and this fact was used to adjust the runup coefficient a so that any predetermined exceedance level for R_{max} could be achieved. For example, by increasing the coefficient a by two standard deviations of the percent error gives R_{max} predictions which would be expected to exceed 97.7 percent of the observed values of R_{max} . This technique produces a logical envelope for the data. Table 2 lists the standard deviation σ of

the percent error which was used in this method and the correlation squared which is the variance explained by the regression equation used to predict R_{max}/H_{mo} .

PART V: CONCLUSIONS AND RECOMMENDATIONS

22. Visual observations of the maximum runup of irregular waves on riprap give reliable values of the maximum elevation of wave uprush. For the two studies considered the time interval of observation was 256 sec. It is difficult for an observer to maintain adequate concentration on the runup process for intervals longer than 256 sec. This interval provides between 100 and 250 runup events at the wave periods tested. Future tests will consider using photogrametric methods to measure irregular wave runup on riprap to increase the time interval of observation and to obtain the entire runup distribution rather than just the maximum value.

23. The runup equations presented appear to be the best available to estimate the approximate upper limit of irregular wave uprush on riprap revetments. Further tests are planned which should produce improved methods to determine the runup characteristics of irregular waves on rough and porous slopes.

REFERENCES

Ahrens, J. P., and McCartney, B. L. 1975 (Jun). "Wave Period Effect on the Stability of Riprap," Proceedings Civil Engineering in the Oceans III, American Society of Civil Engineers, Newark, Delaware, pp 1019-1034.

Ahrens, J. P., and Seelig, W. N. (May) 1980. "Wave Runup on a Riprap Protected Dike," unpublished report to the Detroit District, Detroit, Michigan.

Ahrens, J. P., and Zirkle, K. P. (Jun) 1982. "Riprap Stability Model Tests," unpublished report to the Jacksonville District, Jacksonville, Florida.

Ahrens, J. P., Heimbaugh, M. S., and Davidson, D. D. 1986. "Irregular Wave Overtopping of Seawall/Revetment Configurations, Roughans Point, Massachusetts," Technical Report CERC-86-7, US Army Engineer Waterways Experiment Station, Vicksburg, Mississippi.

Broderick, L. L., and Ahrens, J. P. 1982 (Aug). "Riprap Stability Scale Effects," Technical Report CERC-82-3, Ft. Belvoir, Virginia.

Cornell, C. A., and Benjamin, J. R. 1970. Probability, Statistics, and Decision for Civil Engineers, McGraw-Hill, New York.

Goda, Y. 1975. "Irregular Wave Deformation in the Surf Zone," Coastal Engineering in Japan, Vol 18, pp 13-26.

Goda, Y. 1983 (Sep). "A Unified Nonlinearity Parameter of Water Waves," Report of the Port and Harbor Research Institute, Vol 22, No. 3, pp 3-30, Yokosuka, Japan.

Goda, Y., and Suzuki, Y. 1976. "Estimation of Incident and Reflected Waves in Random Wave Experiments," Procceedings of the Fifteenth International Conference on Coastal Engineering, Hawaii.

Hughes, S. A. 1984 (Dec). "The TMA Shallow-Water Spectrum Description and Application," Technical Report CERC-84-7, US Army Engineer Waterways Experiment Station, Vicksburg, Mississippi.

Seelig, W. N. 1980 (Jun). "Two-dimensional Tests of Wave Transmission and Reflection Characteristics of Laboratory Breakwaters," Technical Report CERC-80-1, US Army Engineer Waterways Experiment Station, Vicksburg, Mississippi.

Shore Protection Manual. 1984. 4th ed. 2 vols, US Army Engineer Waterways Experiment Station, Vicksburg, Miss.Coastal Engineering Research Center, US Government Printing Office, Wahington, DC.

US Army Corps of Engineers. 1985 (Dec). "Estimating Irregular Wave Runup Heights on Rough Slopes, Computer Program: Wavrunup (MACE-14)," CERC CETN-I-37, US Army Engineer Waterways Experiment Station, Vicksburg, Mississippi.

APPENDIX A

SUMMARY OF JACKSONVILLE AND DETROIT DISTRICT TEST CONDITIONS

Table A1

Summary of Jacksonville (SAJ) and Detroit District (NCE) Test Conditions

study design	Test No.	offshore depth cm	wave period T_p sec	offshore Hmo cm	inshore depth d_s cm	estimate inshore Hmo cm	inshore wave length L_p cm	Rmax cm	structure slope cot theta	offshore fronting slope cot alpha	median armor weigh W50 gr	armor unit weight wr gr/cm^3	armor layer thickness r(bar) cm	median weight filter stone gr	filter stone unit weight gr/cm^3	filter layer thickness cm	typical dimensn. armor stone cm	typical dimensn. filter stone cm	armor r(bar) over d50
Detroit	1	36.901	2.753	5.077	11.901	4.945	294.071	11.392	2.00	15.00	187.00	2.65	10.00	18.00	2.65	5.50	4.13	1.89	2.42
Detroit	2	36.901	1.533	6.797	11.901	6.394	159.919	9.392	2.00	15.00	187.00	2.65	10.00	18.00	2.65	5.50	4.13	1.89	2.42
Detroit	3	36.901	1.020	7.348	11.901	6.496	101.704	9.506	2.00	15.00	187.00	2.65	10.00	18.00	2.65	5.50	4.13	1.89	2.42
Detroit	4	36.901	3.821	10.218	11.901	7.544	410.311	24.403	2.00	15.00	187.00	2.65	10.00	18.00	2.65	5.50	4.13	1.89	2.42
Detroit	5	36.901	2.032	9.536	11.901	7.334	215.118	14.897	2.00	15.00	187.00	2.65	10.00	18.00	2.65	5.50	4.13	1.89	2.42
Detroit	6	36.901	1.684	13.171	11.901	7.202	176.742	20.403	2.00	15.00	187.00	2.65	10.00	18.00	2.65	5.50	4.13	1.89	2.42
Detroit	7	45.500	3.282	5.250	20.500	5.099	459.122	12.402	2.00	15.00	187.00	2.65	10.00	18.00	2.65	5.50	4.13	1.89	2.42
Detroit	8	45.500	1.062	7.424	20.500	6.797	132.112	12.192	2.00	15.00	187.00	2.65	10.00	18.00	2.65	5.50	4.13	1.89	2.42
Detroit	9	45.500	1.571	7.700	20.500	7.252	210.219	13.506	2.00	15.00	187.00	2.65	10.00	18.00	2.65	5.50	4.13	1.89	2.42
Detroit	10	45.500	1.954	9.058	20.500	8.644	267.000	17.793	2.00	15.00	187.00	2.65	10.00	18.00	2.65	5.50	4.13	1.89	2.42
Detroit	11	45.500	3.507	9.856	20.500	9.584	491.389	28.308	2.00	15.00	187.00	2.65	10.00	18.00	2.65	5.50	4.13	1.89	2.42
Detroit	12	45.500	2.032	10.710	20.500	10.239	278.362	17.202	2.00	15.00	187.00	2.65	10.00	18.00	2.65	5.50	4.13	1.89	2.42
Detroit	13	45.500	2.032	13.402	20.500	12.274	278.362	22.498	2.00	15.00	187.00	2.65	10.00	18.00	2.65	5.50	4.13	1.89	2.42
Detroit	14	45.500	1.684	15.777	20.500	11.890	227.174	22.993	2.00	15.00	187.00	2.65	10.00	18.00	2.65	5.50	4.13	1.89	2.42
Detroit	15	53.501	3.282	5.747	28.501	5.581	538.626	16.497	2.00	15.00	187.00	2.65	10.00	18.00	2.65	5.50	4.13	1.89	2.42
Detroit	16	53.501	1.148	8.209	28.501	7.638	163.885	14.307	2.00	15.00	187.00	2.65	10.00	18.00	2.65	5.50	4.13	1.89	2.42
Detroit	17	53.501	1.580	12.064	28.501	11.410	243.886	19.393	2.00	15.00	187.00	2.65	10.00	18.00	2.65	5.50	4.13	1.89	2.42
Detroit	18	53.501	1.940	15.004	28.501	14.339	307.701	33.395	2.00	15.00	187.00	2.65	10.00	18.00	2.65	5.50	4.13	1.89	2.42
Detroit	19	53.501	1.620	17.770	28.501	15.691	251.082	26.194	2.00	15.00	187.00	2.65	10.00	18.00	2.65	5.50	4.13	1.89	2.42
Detroit	20	53.501	2.170	14.632	28.501	14.048	347.857	26.403	2.00	15.00	187.00	2.65	10.00	18.00	2.65	5.50	4.13	1.89	2.42
Detroit	21	53.501	4.741	12.687	28.501	12.380	785.372	30.994	2.00	15.00	187.00	2.65	10.00	18.00	2.65	5.50	4.13	1.89	2.42
Detroit	22	53.501	3.200	10.737	28.501	10.420	524.679	26.994	2.00	15.00	187.00	2.65	10.00	18.00	2.65	5.50	4.13	1.89	2.42
Detroit	23	58.299	3.122	5.926	33.299	5.753	550.935	18.898	2.00	15.00	187.00	2.65	10.00	18.00	2.65	5.50	4.13	1.89	2.42
Detroit	24	58.299	1.243	8.155	33.299	7.649	191.863	13.602	2.00	15.00	187.00	2.65	10.00	18.00	2.65	5.50	4.13	1.89	2.42
Detroit	25	58.299	1.533	10.331	33.299	9.779	250.539	17.697	2.00	15.00	187.00	2.65	10.00	18.00	2.65	5.50	4.13	1.89	2.42
Detroit	26	58.299	2.170	14.971	33.299	14.394	373.350	25.794	2.00	15.00	187.00	2.65	10.00	18.00	2.65	5.50	4.13	1.89	2.42
Detroit	27	58.299	1.620	18.419	33.299	17.486	267.762	30.004	2.00	15.00	187.00	2.65	10.00	18.00	2.65	5.50	4.13	1.89	2.42
Detroit	28	58.299	3.241	9.765	33.299	9.486	572.800	27.794	2.00	15.00	187.00	2.65	10.00	18.00	2.65	5.50	4.13	1.89	2.42
Detroit	29	58.299	4.741	15.573	33.299	15.204	847.677	37.700	2.00	15.00	187.00	2.65	10.00	18.00	2.65	5.50	4.13	1.89	2.42
Detroit	30	58.299	2.909	11.081	33.299	10.742	511.541	27.794	2.00	15.00	187.00	2.65	10.00	18.00	2.65	5.50	4.13	1.89	2.42
Detroit	31	63.500	2.753	6.239	38.500	6.047	516.442	17.602	2.00	15.00	187.00	2.65	10.00	18.00	2.65	5.50	4.13	1.89	2.42
Detroit	32	63.500	1.249	9.226	38.500	8.704	202.286	19.202	2.00	15.00	187.00	2.65	10.00	18.00	2.65	5.50	4.13	1.89	2.42
Detroit	33	63.500	1.515	8.308	38.500	7.883	260.949	13.506	2.00	15.00	187.00	2.65	10.00	18.00	2.65	5.50	4.13	1.89	2.42
Detroit	34	63.500	1.816	9.670	38.500	9.249	325.017	20.403	2.00	15.00	187.00	2.65	10.00	18.00	2.65	5.50	4.13	1.89	2.42
Detroit	35	63.500	1.506	12.946	38.500	12.281	259.052	22.898	2.00	15.00	187.00	2.65	10.00	18.00	2.65	5.50	4.13	1.89	2.42
Detroit	36	63.500	4.741	14.381	38.500	14.051	910.031	33.909	2.00	15.00	187.00	2.65	10.00	18.00	2.65	5.50	4.13	1.89	2.42
Detroit	37	63.500	1.620	14.931	38.500	14.211	283.661	24.898	2.00	15.00	187.00	2.65	10.00	18.00	2.65	5.50	4.13	1.89	2.42
Detroit	38	63.500	2.813	8.992	38.500	8.720	528.574	25.108	2.00	15.00	187.00	2.65	10.00	18.00	2.65	5.50	4.13	1.89	2.42
Detroit	39	36.901	1.062	6.683	11.901	6.029	106.610	9.601	2.00	15.00	187.00	2.65	10.00	18.00	2.65	5.50	4.13	1.89	2.42
Detroit	40	36.901	3.460	7.885	11.901	7.525	371.034	18.002	2.00	15.00	187.00	2.65	10.00	18.00	2.65	5.50	4.13	1.89	2.42
SAJ	3	48.812	1.490	NA	23.812	7.544	210.800	9.601	4.00	NA	56.90	2.55	3.24	11.60	2.65	2.50	2.82	1.64	1.15
SAJ	4	48.812	1.440	NA	23.812	5.086	202.600	5.505	4.00	NA	56.90	2.55	3.24	11.60	2.65	2.50	2.82	1.64	1.15
SAJ	8	48.812	1.420	NA	23.812	6.153	199.700	9.906	4.00	NA	56.90	2.55	3.24	11.60	2.65	2.50	2.82	1.64	1.15
SAJ	9	48.812	1.480	NA	23.812	3.181	208.800	5.906	4.00	NA	56.90	2.55	3.24	11.60	2.65	2.50	2.82	1.64	1.15
SAJ	10	44.050	1.390	NA	19.050	10.268	177.000	10.497	4.00	NA	56.90	2.55	3.39	11.60	2.65	2.50	2.82	1.64	1.20
SAJ	11	44.050	1.420	NA	19.050	9.430	181.400	10.306	4.00	NA	56.90	2.55	3.32	11.60	2.65	2.50	2.82	1.64	1.18
SAJ	12	44.050	1.420	NA	19.050	8.115	181.800	8.592	4.00	NA	56.90	2.55	3.13	11.60	2.65	2.50	2.82	1.64	1.11
SAJ	13	44.050	1.470	NA	19.050	6.001	189.400	7.201	4.00	NA	56.90	2.55	3.09	11.60	2.65	2.50	2.82	1.64	1.10
SAJ	25	48.812	1.450	NA	23.812	8.725	204.700	13.506	3.00	NA	66.00	2.55	4.45	11.60	2.65	2.50	2.96	1.64	1.51
SAJ	26	48.812	1.460	NA	23.812	6.401	205.900	9.792	3.00	NA	66.00	2.55	4.14	11.60	2.65	2.50	2.96	1.64	1.40
SAJ	27	48.812	1.420	NA	23.812	3.143	199.700	7.106	3.00	NA	66.00	2.55	4.11	11.60	2.65	2.50	2.96	1.64	1.39
SAJ	30	48.812	1.420	NA	23.812	8.001	198.900	13.202	3.00	NA	66.00	2.55	4.04	11.60	2.65	2.50	2.96	1.64	1.37
SAJ	31	44.050	1.410	NA	19.050	10.382	180.300	12.706	3.00	NA	64.80	2.55	3.15	11.60	2.65	2.50	2.94	1.64	1.07
SAJ	32	44.050	1.390	NA	19.050	9.639	177.400	11.601	3.00	NA	64.80	2.55	3.16	11.60	2.65	2.50	2.94	1.64	1.08
SAJ	33	44.050	1.460	NA	19.050	8.325	186.800	10.592	3.00	NA	64.80	2.55	3.14	11.60	2.65	2.50	2.94	1.64	1.07
SAJ	34	44.050	1.410	NA	19.050	6.210	180.300	9.601	3.00	NA	64.80	2.55	2.85	11.60	2.65	2.50	2.94	1.64	0.97
SAJ	35	44.050	1.460	NA	19.050	2.991	186.800	5.601	3.00	NA	64.80	2.55	3.17	11.60	2.65	2.50	2.94	1.64	1.08
SAJ	36	44.050	1.390	NA	19.050	10.516	177.700	13.297	3.00	NA	64.80	2.55	3.21	11.60	2.65	2.50	2.94	1.64	1.09
SAJ	37	44.050	1.420	NA	19.050	9.544	181.000	12.002	3.00	NA	64.80	2.55	3.00	11.60	2.65	2.50	2.94	1.64	1.02
SAJ	38	44.050	1.400	NA	19.050	8.192	178.100	11.697	3.00	NA	64.80	2.55	3.12	11.60	2.65	2.50	2.94	1.64	1.06
SAJ	43	48.812	1.460	NA	23.812	8.668	207.100	13.506	3.00	NA	64.50	2.55	2.67	11.60	2.65	2.50	2.94	1.64	0.91
SAJ	44	48.812	1.440	NA	23.812	6.496	202.600	10.001	3.00	NA	64.50	2.55	2.63	11.60	2.65	2.50	2.94	1.64	0.90
SAJ	45	48.812	1.440	NA	23.812	3.124	203.000	6.096	3.00	NA	64.50	2.55	2.54	11.60	2.65	2.50	2.94	1.64	0.86
SAJ	46	44.050	1.440	NA	19.050	10.344	185.400	12.992	3.00	NA	63.30	2.55	3.08	11.60	2.65	2.50	2.92	1.64	1.06
SAJ	47	44.050	1.460	NA	19.050	9.601	187.600	12.592	3.00	NA	63.30	2.55	2.94	11.60	2.65	2.50	2.92	1.64	1.01
SAJ	48	44.050	1.400	NA	19.050	8.115	179.600	11.601	3.00	NA	63.30	2.55	2.74	11.60	2.65	2.50	2.92	1.64	0.94
SAJ	49	44.050	1.440	NA	19.050	6.134	184.300	8.192	3.00	NA	63.30	2.55	2.55	11.60	2.65	2.50	2.92	1.64	0.87
SAJ	50	44.050	1.430	NA	19.050	4.610	182.800	7.296	3.00	NA	63.30	2.55	2.71	11.60	2.65	2.50	2.92	1.64	0.93